

Climate change impacts and vulnerability of the southern populations of *Pinus nigra* subsp. *salzmannii*

JUAN CARLOS LINARES^{1,2} and PEDRO ANTONIO TÍSCAR³

¹ Departamento de Sistemas Físicos, Químicos y Naturales, Universidad Pablo de Olavide. Ctra. Utrera km. 1, 41002 Sevilla, Spain

² Corresponding author (jclincal@upo.es)

³ Centro de Capacitación y Experimentación Forestal, 23470 Cazorla, Spain

Received January 26, 2010; accepted May 5, 2010; published online June 3, 2010

Summary The understanding of regional vulnerability to climate change in Mediterranean mountain forests is not well developed. Climate change impacts on tree growth should be strongly related to the steep environmental gradients of mountainous areas, where a temperature-induced upward shift of the lower elevation limit is expected, particularly amongst drought-sensitive species. Trees will adapt not only to changes in mean climate variables but also to increased extreme events such as prolonged drought. In this paper, we investigate the sub-regional temperature and precipitation trends and measure the basal area increment (BAI) in *Pinus nigra* subsp. *salzmannii* (Dunal) Franco. Significant differences related to altitudinal and latitudinal gradients and stand-age structure were found in response to long-term trends in climate dryness. Old trees growing at higher elevations showed similar extreme drought sensitivity but maintained almost steady BAI. Declining BAI found in trees at lower elevations and drier sites may imply a higher vulnerability to temperature-induced drought stress, suggesting an impending growth decline and an enhanced die-off risk. Our results illustrate how the effects of long-term warming and short-term drought on tree BAI are influenced by both site conditions and mean stand age in a drought-sensitive Mediterranean pine.

Keywords: basal area increment, drought, linear mixed models, mediterranean forests.

Introduction

Global climate observations show the existence of a warming trend (IPCC 2007) that is expected to modify the growth and distribution of tree species. Trees are known to be sensitive to temperature increases (Adams et al. 2009), but uncertainties still remain about forest vulnerability to climate change (Lindner et al. 2009). Recent papers propose that tree growth vulnerability to climate change could be assessed as a function of the climate impacts

and tree growth sensitivity and adaptive capacity (Lindner et al. 2009). Hence, climate effects on tree growth will depend on the specific climate changes at the regional scale, tree species' inherent sensitivity and their ability to cope with the impacts (Linares et al. 2010). Although many studies have investigated tree growth patterns in relation to long-term climate trends, much less attention has been given to comparisons of tree vulnerability across sites within a given system (but see Schröter et al. 2005).

Different researchers have found either enhancement or decline responses in radial growth to increasing temperatures (Boisvenue and Running 2006, Andreu et al. 2007). Many studies have focused on tree growth responses to gradual changes; however, the effects of climate variability and extreme events are expected to be much more critical to tree growth (Loustau et al. 2005). An increase in temperature alone would be beneficial for some populations, but an interaction with other climate- or site-related factors could alter the response (Keeling et al. 1996). Higher temperatures extend the growing season and may increase photosynthesis, particularly at higher elevations (Wullschlegel et al. 2002). For instance, warming has been linked to an extension of the growing period during the 20th century in temperate European forests (Peñuelas and Filella 2001). However, where water availability restricts productivity, drought-induced growth decline is more likely, especially if precipitation does not increase or rainfall decreases during the growing period (Loustau et al. 2005, Martínez-Vilalta et al. 2008).

The study of how water stress interacts with local site conditions to affect conifer tree growth could be essential to understanding the response of many key forest ecosystems to climate change (Camarero et al. 1998, Deslauriers and Morin 2005, Vaganov et al. 2006). Assessment of radial growth variability under contrasting climatic conditions may serve to gauge tree vulnerability in the face of increasing climatic variability. However, conifer climate–growth relationships have mainly been investigated in temperate, boreal and high-altitude species (Antonova et al. 1995, Camarero et al.

1998, Deslauriers et al. 2003, Rossi et al. 2006b, Ko Heinrichs et al. 2007). In contrast, little is known about secondary growth in Mediterranean mountain conifers, which are subjected to very unpredictable climatic and water stress constraints as well as low winter temperatures (but see Andreu et al. 2007, De Luis et al. 2007, Linares et al. 2009a).

In addition to temperature increase, changes in amounts and patterns of precipitation are likely subject to high uncertainty at local and regional scales (Lindner et al. 2009). Regional climate simulations predict a decrease in annual mean precipitation for the Mediterranean Basin (Sumner et al. 2003, IPCC 2007). Precipitation variability could be particularly important because extreme events, such as extended droughts, could have much more drastic consequences on tree growth and survival than gradual changes in the average climate conditions (Loustau et al. 2005, Granier et al. 2007). Thus, if the frequency of extreme droughts in Mediterranean areas increases in the future, it could lead to a reduction in forest productivity and changes in species composition (Martínez-Vilalta et al. 2008, Allen et al. 2009). Nonetheless, tree growth responses to long-term temperature trends and extreme drought events are currently poorly understood (but see Orwig and Abrams 1997, He et al. 2005, Pichler and Oberhuber 2007, Adams et al. 2009).

A positive effect of temperature increase is not expected in Mediterranean forests because warming effects on evapotranspiration can result in soil water deficits (Pereira and Chaves 2001, Sabaté et al. 2002, Linares et al. 2009a). Indeed, mountainous areas of the Mediterranean Basin may experience somewhat higher increases in temperature compared with the surrounding regions (IPCC 2007), which could increase the vulnerability of the Mediterranean mountain forests to climate change. A quantification of radial growth responses to climatic constraints, site conditions and stand-age structure will allow the growth and persistence of Mediterranean mountain conifers under current climatic scenarios to be evaluated.

The degree to which trees were affected by climate change, either adversely or beneficially, was assessed using climate–growth relationships derived from long- and short-term temperature and precipitation trends at a sub-regional scale. The degree to which trees were susceptible to adverse effects of climate change (i.e., vulnerability) was summarized as a function of the most critical climatic trends and drought sensitivity. We investigated sub-regional temperature and precipitation trends and radial growth patterns of *Pinus nigra* subsp. *salzmannii* (Dunal) Franco (*P. nigra*, hereafter) in the wider southernmost distribution area of this Mediterranean pine (i.e., Sierra de Cazorla, Segura y las Villas Natural Park; Tíscar 2007). *P. nigra* has been found to be a drought-sensitive species (e.g., Richter et al. 1991, Fernández et al. 1996, Martín-Benito et al. 2007), which makes it susceptible to the increase in temperature and decrease in precipitation already observed in southeast Spain and predicted by climate change models (Sumner et al. 2003). Our specific aims were:

(i) to describe the spatial and temporal patterns of temperature and precipitation in the southernmost distribution area of *P. nigra*; (ii) to quantify the climate–growth relationship of *P. nigra* in its southernmost distribution range; and (iii) to quantify the drought sensitivity and basal area increment (BAI) trends of *P. nigra*'s radial growth. We hypothesize that across-site conditions may greatly modulate tree vulnerability to climate change.

Materials and methods

Field sampling and dendrochronological methods

This study was carried out in the Sierra de Cazorla, Segura y las Villas Natural Park during the summer of 2005. The main soil types in the region are based on a dolomite and calcareous bedrock. These substrates and the Mediterranean climate that consists of distinct wet and dry seasons, create leptosols (rendzinas) on higher slopes and luvisols on flat terrain with alluvial and colluvial deposits (Alejano and Martínez 1996).

We selected 10 study sites on a map that covered the altitudinal and latitudinal gradients of *P. nigra* natural stands present in the Natural Park. The difference in altitude between the highest and lowest sites was 803 m, and the most distant sites were 67.5 km apart (see Table 1).

At each site, we roughly marked a plot (ca. 2–4 ha, depending on the geomorphology and stand structure) and selected the 10 apparently largest diameter and most dominant trees (Figure 1). We sampled dominant trees, avoiding those with asymmetrical growth and non-circular bole. Each tree was measured for stem circumference to obtain the diameter at breast height (1.3 m from the base, d.b.h.). Then, one core per tree at d.b.h. was extracted perpendicular to the terrain slope. Given that the studied stands have not been strongly disturbed by logging or fires within the last century, few dominant trees need to be sampled to obtain a reliable growth pattern related to the regional climatic signal. In addition, since special care and considerable time–effort were applied to meet the above criteria, a single core per tree was considered representative of that tree for dendrochronological analyses (Fritts et al. 1991). Moreover, just after collection, each sample was visually examined in the field for scars, wood rot and other anomalies, in which case it was discarded and the tree re-sampled or excluded. Two trees from plot PP and one tree from plot NC were excluded, and four trees from three different plots (VA, VT and PT) were re-sampled. Using a 40-cm increment borer, we were able to reach the heartwood centre in 84% of the sampled trees (BT 10/10, YE 8/10, PA 9/10, CI 10/10, NC 8/10, CM 7/10, VA 10/10, PT 8/10, BG 6/10, PP 8/10).

Cores were sanded and visually cross-dated, and their ring-width series were measured to the nearest 0.001 mm with the help of a stereomicroscope mounted above a Velmex 'TA' System device linked to a computer. Cross-dating quality was checked using COFECHA (Holmes 1983). Tree-ring

Table 1. Mean characteristics of the *Pinus nigra* subsp. *salzmannii* populations studied in the Sierra de Cazorla, Segura y las Villas Natural Park. Minimum/mean/maximum d.b.h. and age are represented in the last two rows. Values are means \pm SE.

Plot	PP	CI	NC	BG	VA	CM	PT	PA	YE	BT
Latitude (N)	37°49'	37°53'	37°54'	37°55'	37°55'	38°00'	38°03'	38°06'	38°15'	38°21'
Longitude (W)	2°58'	2°58'	2°52'	2°48'	2°57'	2°40'	2°44'	2°52'	2°39'	2°33'
Elevation (m a.s.l.)	1819 \pm 21	1211 \pm 71	1435 \pm 18	1699 \pm 25	1133 \pm 36	1794 \pm 16	1633 \pm 20	1016 \pm 11	1600 \pm 21	1233 \pm 19
Slope (%)	24 \pm 4	30 \pm 5	25 \pm 5	26 \pm 3	20 \pm 7	18 \pm 6	23 \pm 5	29 \pm 7	21 \pm 1	31 \pm 4
Aspect	E-NE	E-NE	N-NE	O-NO	N-NE	O-NO	S-SO	N-NO	E-SE	N-NO
Mean temperature (°C)	8.95	11.52	10.45	9.38	11.95	9.03	9.63	12.64	9.76	11.41
Total annual precipitation (mm)	1393	1172	1219	1278	1123	1235	1149	939	975	791
d.b.h. of sampled trees (max/mean/min, cm)	52/61/80	55/62/70	59/64/74	64/80/117	64/74/82	65/75/88	65/74/83	61/72/80	56/61/68	56/69/84
Age at d.b.h. of sampled trees (max/mean/min, years)	97/242/398	125/145/174	123/222/284	115/205/282	101/138/207	95/223/331	100/156/248	108/126/174	72/207/301	136/174/214

widths were converted to BAI because it is more closely related to biomass increment. When a wood core did not reach the pit, we calculated BAI values as follows. First, we calculated the tree stem radius (R) from its stem circumference (C) measured at 1.3 m from the base, as $R = C/2\pi$. Then, we obtained the radius inside bark (RIB) as the difference between R and the bark thickness measured on the core. The difference between RIB and the core length (L) gives the radius of the stem just prior to the formation of the first tree ring captured by the core. Thus, the stem basal area at that time (BA_0) can be estimated as:

$$BA_0 = \pi * (RIB - L)^2 \quad (1)$$

The stem basal area by the end of the following year (the year of formation of the oldest tree ring in the core) can be calculated as:

$$BA_1 = \pi * (RIB - L + TRW_1)^2 \quad (2)$$

where TRW_1 is the measured width of the oldest ring in the core. Therefore, the first BAI value in our time series is:

$$BAI_1 = BA_1 - BA_0 = \pi * (RIB - L + TRW_1)^2 - \pi * (RIB - L)^2$$

the second one is:

$$BAI_2 = BA_2 - BA_1 = \pi * (RIB - L + TRW_1 + TRW_2)^2 - \pi * (RIB - L + TRW_1)^2$$

and so on.

Drought sensitivity was defined as the degree to which tree growth is affected by an extreme drought event. Based on climatic results, we selected three extreme drought events (years with total precipitation at least two standard deviations below the mean) in the 20th century, separated by at least 10 years. Then, drought sensitivity (DS) was estimated for each tree as the mean BAI during the drought event, plus the year after the drought occurred, divided by the mean BAI during the 10 years prior to the drought:

$$DS = \frac{\text{mean}(BAI_D + BAI_{D+1})}{\text{mean}(BAI_{D-10})} \quad (3)$$

where BAI_D is the BAI in the year the drought occurred, BAI_{D+1} is the BAI in the year after the drought occurred, and BAI_{D-10} is the BAI of the 10 years prior to the drought. Thereafter, the degree to which trees are susceptible to adverse effects of climate change (i.e., vulnerability) was discussed as a function of key climate trends and drought sensitivity.

Climatic data

To estimate robust and long-term regional climatic records, local data from 39 meteorological stations available inside the Natural Park were combined into a regional mean for



Figure 1. Old *Pinus nigra* subsp. *salzmannii* growing at 1870 m in the Sierra de Cazorla, Segura y las Villas Natural Park. This figure appears in color in the online version of *Tree Physiology*.

the period of 1920–2004 (see Appendix, Table A1, available as Supplementary Data at *Tree Physiology* Online). For each station, monthly variables (mean temperature, total precipitation) were transformed into normalized standard de-

viations to give each station the same weight in calculating the average values for each month and year. To combine the data from each station, we used the MET routine from the Dendrochronology Program Library (Holmes 1992). Regional means were used instead of those available from individual weather stations because of the lack of stations or long-term data set for several sites and the limited representation of local stations in this mountain area. The annual water budget was obtained from the sum of the monthly differences between the precipitation data and the potential evapotranspiration estimated by a modified version of the Thornthwaite method (Willmott et al. 1985). Annual means were based on data from September of the previous year to August of the current year.

Temporal trends of monthly mean temperature and monthly total precipitation were estimated using the Mann–Kendall test (Mann 1945, Kendall 1975). Mann–Kendall tests (hereafter MK) are non-parametric tests for the detection of trends in a time series. These tests are widely used in environmental science because they are simple and robust and can cope with missing values and values below the detection limit. For each time series element x_i ($1, 2, \dots, n$), the number (n_i) of x_j elements lower than x_i ($x_j < x_i$) and previous in time ($j < i$) are counted. Then, the MK statistic for the time series $\{Z_k, k = 1, 2, \dots, n\}$ is defined as

$$T = \sum_{j < i} \text{sgn}(Z_i - Z_j) \quad (4)$$

where

$$\text{sgn}(x) \begin{cases} 1, & \text{if } x > 0 \\ 0, & \text{if } x = 0 \\ -1, & \text{if } x < 0 \end{cases}$$

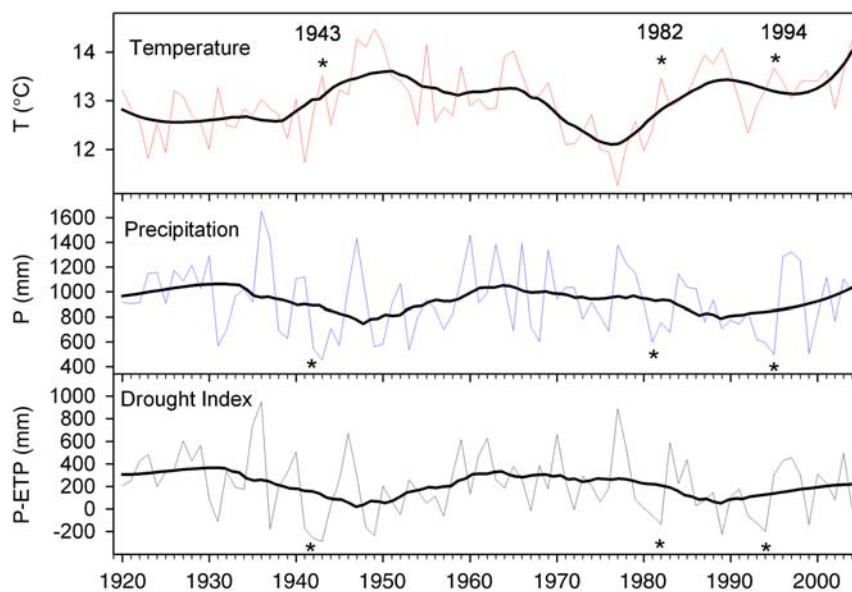


Figure 2. Regional mean temperature, precipitation and drought index (precipitation minus evapotranspiration) for 1920–2004. Asterisk indicates extreme drought events selected (1943, 1982 and 1994) to quantify drought sensitivity. This figure appears in color in the online version of *Tree Physiology*.

If no ties between the observations are present and no trend is present in the time series, the test statistic is asymptotically normally distributed with mean $E(t) = 0$, independent of the distribution function of the data. The statistic $E(T)$ is defined as:

$$E(T) = \frac{T - \langle T \rangle}{\sqrt{\text{Var}(T)}} \quad (5)$$

where $\langle T \rangle$ and $\text{var}(T)$ are computed as

$$\langle T \rangle = \frac{n(n-1)}{4}$$

and

$$\text{var}(T) = \frac{n(n-1)(2n+5)}{18}$$

The null hypothesis assumes that the trend is zero, and it is rejected if $E(T)$ is higher in absolute value than 1.96 for a two-tailed test at 95% significance or 2.58 at 99% significance. The $E(T)$ sign indicates whether the trend is positive or negative. The MK test also allows the ascertainment of a summarized trend of the data by estimation of a multivariate analysis of the monthly data, which was interpreted in this paper as a summarized annual trend (Libiseller and Grimvall 2002). The analyses were performed using a free application downloaded from http://www.etsm.slu.se/ShowPage.cfm?OrgenhetSida_ID=8144.

When significant trends were obtained from MK, the rates of change of the climatic variables were estimated by obtaining their slopes from simple linear regression.

Data analyses and modelling: linear mixed-effects model

Based on previous dendroecological studies focused on *P. nigra* in Spain (e.g., Richter et al. 1991, Fernández et al. 1996, Martín-Benito et al. 2007) and preliminary correlation analyses, significant monthly temperature and precipitation ($P < 0.05$ from the revised response function and correlation analyses) were used as potential long-term explanatory variables of the BAI in each plot. To model BAI as a function of temperature and precipitation, we fitted linear mixed-effects models (LMEM) using the nlme package in R software (R Development Core Team 2010). Monthly temperature and precipitation from the previous September to the current December were included as fixed effects, and each tree was included as a random effect. The covariance parameters were estimated using the restricted maximum likelihood method, which obtains estimates of parameters by minimizing the likelihood of residuals from fitting the fixed effects portion of the model (Zuur et al. 2009). Several significant variables were correlated (for instance, March, April and May temperatures; June and July temperatures; May and June precipitation); in those cases, we selected the one with higher explained variance (R^2).

Statistical analyses

The BAI values were tested for autocorrelation and normality prior to LMEM analyses. The drought sensitivity values were tested for homogeneity of variance and for the assumption of compound symmetry of the variance–covariance matrix using the Bartlett–Box F -test and the Mauchly criterion, respectively. The drought sensitivity data were then log-transformed to follow homoscedasticity. A repeated-measures multivariate analysis of variance (MANOVA) was used to compare BAI ('manova' and 'summary.manova' R codes; von Ende 2001). Because our main interest was to test the site effect and its interaction with stand structure, the between-subject factor was each plot, whereas tree age (at d.b.h.) and tree size (d.b.h.) were considered as covariates. For drought sensitivity analysis, the different drought years were regarded as the within-subject factor. We used the Greenhouse–Geisser statistic to adjust F -tests. Paired comparisons were corrected using Bonferroni adjustment. The MANOVA was calculated using R software (R Development Core Team 2010).

Results

The altitudinal gradient for mean annual temperature (the adiabatic lapse rate) decreased linearly by 0.64 °C for every 100 m of elevation ($y = -0.0064x + 19.46$; $R^2 = 0.71$, $P < 0.0001$; $n = 25$, range 577–1474 m a.s.l.; see Appendix). The estimated mean annual temperatures ranged from 8.95 to 12.64 °C in the study sites (Table 1). The annual precipitation in the study area decreased northward by ~90 mm for every 10 km ($y = -0.009x + 38,973$, expressed in UTM units; $R^2 = 0.35$, $P < 0.01$; $n = 36$, range 37°50'–38°23' N latitude; see Appendix). The variance that was unexplained by the latitudinal gradient was significantly correlated with elevation, which yielded an upward increase in annual precipitation by ~84 mm for every 100 m of elevation ($y = 0.8404x - 846.72$, in mm, detrending the latitude effect; $R^2 = 0.76$, $P < 0.001$; $n = 36$, range 540–1680 m elevation; see Appendix). The estimated annual precipitation ranged from 1393 to 939 mm in the study sites (Table 1).

The regional mean temperature, precipitation and drought index (precipitation minus evapotranspiration) for 1920–2004 are shown in Figure 2. Drought events registered in 1943, 1982 and 1994 were selected to test tree drought sensitivity. The MK test showed a significant increase in mean annual temperature, enhanced since 1970 (+0.41 °C since 1970, Table 2, see Appendix); the months of March to June yielded the higher temperature increases for the period spanning 1970–2004, whereas some autumn months showed cooling trends but were not statistically significant. The precipitation trend showed a more complex pattern, with both significant negative (January, March and June) and positive (September) trends (see Table 2 and Appendix). On average, the total annual precipitation decreased by about 77 mm over

Table 2. Temporal trend of monthly mean temperature and monthly total precipitation estimated by the Mann–Kendal test. Significance is noted as *** $P < 0.001$; ** $P < 0.01$; * $P < 0.05$; and *m*, $P < 0.10$. The trends (slopes) of the significant months were estimated by linear least squares regression.

Time span Month	Temperature					Precipitation		
	1920–2004		1970–2004			1920–2004		1970–2004
	MK-Stat		MK-Stat	Slope (°C/decade)	MK-Stat	MK-Stat	Slope (mm/decade)	
January	-0.49		-0.38		-0.83	-1.63	<i>m</i> -15.44	
February	1.71	<i>m</i>	1.53		-1.64	-1.37		
March	2.89	***	4.47	***	1.27	-2.52	* -1.85	
April	1.40		2.94	***	0.81	0.36	0.21	
May	1.74	<i>m</i>	2.51	**	0.75	0.43	0.11	
June	2.36	**	3.28	***	0.92	-0.79	-2.09	
July	0.97		0.80		0.47	-1.03		
August	-1.21		1.29		0.44	-0.94		
September	-0.61		-1.26		0.52	2.07	* 10.57	
October	-0.76		0.61		0.82	1.20		
November	0.39		-0.18		-1.03	0.71		
December	0.45		0.67		-0.35	-0.50		
Combined test								
Year	1.74	<i>m</i>	2.89	***	0.41	-0.93	-1.13	

the 1970–2004 period, which represents an approximate 9% reduction in the annual total precipitation.

All sampled trees were of similar size (~70 cm d.b.h.); however, tree age and radial growth showed significant differences (Table 1). The time span of the chronologies varied from ~100 to 400 years (data not shown); the mean stand age significantly correlated with elevation, with the older stands located above 1500 m. The BAI characteristics of the study plots are shown in Table 3. On average, the mean BAI during the second half of the 20th century was positively correlated with elevation, except for the higher elevation plot PP. The mean BAI was below 17 cm²year⁻¹ for stands growing below 1300 m for the 1995–2004 span, while it was near 19 cm²year⁻¹ for stands above 1400 m (except for PP and YE stands). Within stands, the mean inter-series correlation was higher at high elevations (ranging from 0.4–0.5 below 1500 m to 0.6–0.7 above 1700 m; Table 3). At tree level, the most significant relationship was a lower mean growth as tree age increased (mean BAI = 35.34 exp(-0.0038 * age); $R^2 = 0.38$; $P < 0.001$; $n = 100$).

Mean BAI showed significant positive autocorrelation among consecutive years (lag = 1); however, monthly temperature showed a similar autocorrelation pattern, which could explain BAI autocorrelation; therefore, we retained raw BAI data (see Appendix). Monthly variables selected for the climate–growth model appear in Table 4, as does their relative weight based on the regression coefficients from LMEM (as raw climate data were transformed into normalized standard deviations, the correlation coefficients are directly comparable). The climate–growth model explained, on average, 38% of the BAI variance (15–56%), but the integrity of the fitting was unrelated to elevation, land use or stand age (Figure 3). Temperature had a negative effect on BAI, with the exception of February, in which positive effects were seen

on five stands (Table 4). May temperature was the most strongly correlated variable, followed by July temperature; on average, the effect of the temperature in October was stronger in the previous year than in the growing year. Precipitation (January and May) explained less variance than temperature for all sites.

Drought sensitivity was similar at both tree and stand levels (Figure 4); on average, the BAI during extreme drought events dropped by about 40% (between 20 and 60%). The studied trees showed a declining growth trend for 7 of the 10 stands (Figure 5). PP and BG showed steady mean growth, while only NC had increased BAI in the 20th century. The mean stand age was strongly correlated with BAI trends (Figure 6). Older stands showed lower BAI declines during the 20th century ($R^2 = 0.67$; $P = 0.004$; $n = 10$). However, within stands, tree-level, age and BAI trends did not show significant patterns. Although the mean stand age rose following the altitudinal gradient (Table 1), BAI trends did not significantly correlate with the elevation ($R^2 = 0.30$; $P = 0.10$; $n = 10$), mean temperature ($R^2 = 0.32$; $P = 0.08$; $n = 10$) or mean precipitation ($R^2 = 0.23$; $P = 0.16$; $n = 10$).

Discussion

The latest climate change scenario projections for Europe predict that by 2100, the annual mean temperatures will increase by 3–4 °C (4–5 °C in summer and 2–3 °C in winter) in parts of the Mediterranean region. Yearly rainfall is expected to drop by up to 20% of current annual precipitation (up to 50% less in summer), whereas winter precipitation is expected to increase (IPCC 2007). Our results support a 20th century warming trend in the study area, mainly between the months of February and June. After 1970, the temperature

Table 3. Radial growth characteristics of the study plots. Values are the means \pm SE from 10 trees per tree was studied. Trends are expressed as the slopes of simple linear regressions. The mean radial growth expressed as tree-ring width and basal area increment (BAI) are shown for the 1950–2004 and 1995–2004 periods. Whiting plot correlations (r Pearson) are also shown for these two periods.

Plot	PP	CI	NC	BG	VA	CM	PT	PA	YE	BT
BAI trend 1920–2004 ($\text{cm}^2 \text{ 10 year}^{-1}$)	-0.10 ± 0.24	-1.06 ± 0.31	0.51 ± 0.29	0.05 ± 0.29	-1.08 ± 0.28	-0.56 ± 0.91	-0.80 ± 0.38	-1.75 ± 0.47	-0.41 ± 0.17	-0.66 ± 0.37
BAI (cm^2) 1950–2004	11.92 ± 1.11	17.03 ± 1.22	18.91 ± 2.07	22.23 ± 1.88	16.10 ± 1.11	23.78 ± 3.55	18.13 ± 1.60	17.80 ± 2.09	17.27 ± 2.35	17.61 ± 1.00
BAI (cm^2) 1995–2004	12.27 ± 1.78	16.99 ± 1.99	19.05 ± 2.49	20.68 ± 1.90	14.83 ± 0.92	21.56 ± 3.16	19.45 ± 1.96	15.18 ± 1.75	14.03 ± 1.46	14.84 ± 0.57
BAI correlation 1950–2004	0.60 ± 0.04	0.42 ± 0.05	0.46 ± 0.06	0.66 ± 0.02	0.45 ± 0.03	0.65 ± 0.06	0.51 ± 0.06	0.52 ± 0.06	0.51 ± 0.06	0.59 ± 0.03
BAI correlation (r Pearson) 1995–2004	0.52 ± 0.08	0.59 ± 0.04	0.43 ± 0.06	0.79 ± 0.04	0.67 ± 0.05	0.63 ± 0.12	0.62 ± 0.08	0.47 ± 0.07	0.60 ± 0.04	0.73 ± 0.05

increase pattern was very consistent for the months between March and June, yielding an annual mean temperature increase of $1.23 \text{ }^\circ\text{C}$ ($3.81 \text{ }^\circ\text{C}$ for March and $2.76 \text{ }^\circ\text{C}$ for June) between 1970 and 2000. Extrapolation of this rate yields a predicted warming of about $4 \text{ }^\circ\text{C}$ in the next century. The precipitation trend showed a more complex pattern, with both significant negative (January, March and June) and positive (September) trends (Table 2). On average, the total annual precipitation decreased by about 77 mm between 1970 and 2000, which represents a reduction in total annual precipitation of approximately 9%. Extrapolation of this rate yields a predicted reduction of approximately 28% in the total annual precipitation for the next century.

Sites currently limited by temperature (i.e., forests at higher elevations) could generally expect growth increases as a result of warming (Tardif et al. 2003, Büntgen et al. 2007). However, the productivity of Mediterranean mountain tree species might be limited by both short growing periods and summer droughts (Férez et al. 1996, Lebourgeois 2000, Martínez-Vilalta et al. 2008). Increasing temperature (Figure 2) could extend the available growing period (Wullschlegel et al. 2002, Boisvenue and Running 2006); however, simultaneous increase in drought events may reduce the amount of time the trees are able to keep their stomata open, therefore reducing carbon uptake and shortening the time span for tree growth (McDowell et al. 2009). Our results support a positive effect of winter temperature on some high-elevation stands, which yielded steady BAI rates over the study period (PP and BG; Table 3, Figure 5). Only one stand showed a significantly positive BAI trend (NC), which was also strongly related to February temperatures (49.01% of relative weight in the climate–growth model, Table 4). Notably, these three stands showing steady or positive BAI trends have a mean annual precipitation above 1200 mm (Table 1). Moreover, drier high-elevation stands from the northern half of the study area (such as PT and YE, see Table 1), did not show a temperature-related BAI increase, which suggests that the positive winter temperature effect is restricted to wetter sites. Lagged negative response to previous year October temperatures was found in four plots (BG, VA, PT and BT; see Table 4). Lower BAI after warm Octobers suggests temperature-induced drought stress, which could reduce carbohydrate accumulation and the size of the dormant cambial zone formed during the previous autumn (Richter et al. 1991, Férez et al. 1996, Martín-Benito et al. 2007).

Stand management might also interact with climate–growth responses, as high-elevation stands showing BAI declines (i.e., PT, CM and YE) also showed a common pattern of sudden BAI releases and suppressions (Figure 3), which could be related to past logging and pruning. Nevertheless, the percentage of BAI variance explained by the climate–growth function was high for the stands CM and YE (Table 4), likely because they were exposed to sunnier conditions, like stand PT. However, trees sampled in PT had been pruned for tar making in the past, which could account for its

Table 4. Relative contribution to the climate–growth model of the seven climatic variables included as predictors for the period 1920–2004. Significant variables are presented in bold. T Oct-1, Temperature of the prior October; T Feb, temperature of current February; T May, temperature of current May; T Jul, temperature of current July; T Oct, temperature of current October; P Jan, precipitation of current January; P May, precipitation of current May. (+)/(-) symbols indicate a positive/negative relationships between the month and the BAI. The relative importance is expressed as the percentage. The variance explained (%) by LMEM is also noted.

Population	Relative contribution to climate–growth model (%)							Total variance explained (%)
	T Oct-1(-)	T Feb(+)	T May(-)	T Jul(-)	T Oct(-)	P Jan(+)	P May(+)	
PP	3.14	5.08	27.84	56.71	5.15	1.48	0.60	15.04
CI	0.02	1.67	58.82	29.20	0.83	2.84	6.62	30.93
NC	0.02	49.01	17.78	4.74	3.89	0.69	23.89	47.82
BG	27.46	28.15	3.30	23.41	3.46	14.22	0.00	43.44
VA	27.46	28.15	3.30	23.41	3.46	14.22	0.00	29.88
CM	1.76	0.19	48.67	0.06	2.67	44.02	2.63	48.54
PT	34.80	0.38	1.31	51.84	7.69	0.57	3.42	30.88
PA	0.81	0.32	47.14	35.38	1.90	13.84	0.60	46.25
YE	0.04	0.88	63.13	19.00	2.10	1.10	13.74	56.11
BT	14.43	3.98	47.98	24.16	0.88	0.23	8.35	27.43

low percentage of explained variance compared with stands CM and YE.

In lower elevation stands, rising spring temperatures and decreasing rainfall from December to March and from June to August will magnify *P. nigra* drought stress (Férez et al. 1996, Lebourgeois 2000) and growth decline. This hypothesis is supported by our results (Figures 2, 3 and 5) and also by short- and long-term studies on other temperate mountain conifers. Significant radial growth reductions in response to severe droughts have been previously observed by Eilmann et al. 2006 in *Pinus sylvestris*. The stem growth of this pine has increased during the 20th century in Catalonia (NW Spain), but increasing temperatures have already had negative impacts on drier sites (Martínez-Vilalta et al. 2008). Climate warming and increasing water stress seem to be the main causes of growth decline in *Abies alba* forests near the southern limit of the species distribution (Macías et al. 2006) and should also lead to a severe BAI reduction in *Abies pinsapo* according to dendrochronological studies (Linares et al. 2009b).

Radial growth is the result of cambium activity, which mainly depends on the whole plant's water and carbon balance and the external climatic conditions. Severe water stress affects processes related to stem growth dynamics in conifers, including carbon sink–source trade-offs within the tree (Vaganov et al. 2006, McDowell et al. 2009). Temperature-induced drought stress may alter the partitioning of newly fixed carbon in such a way that less carbon is diverted for secondary growth (Tognetti et al. 2000, Pichler and Oberhuber 2007, Linares et al. 2010), or more fixed carbon is lost through respiration (Laureano et al. 2008). *P. nigra* trees became increasingly vulnerable to drought, as reflected in the low BAI values during drier periods (Figures 4 and 5). Long-term drought stress could impose further challenges to overcoming drought events (Tiscar 2007), such as a requirement for superior carbon balance when faced with the need to

recover from drought or the loss of needles induced by insect herbivores (Franklin et al. 1987). Increasing temperature raises the vapour pressure deficit and evaporation to the atmosphere. Drier conditions induce stomatal closure to reduce water loss through transpiration. Since photosynthetic rate is reduced by stomatal closure, carbon uptake will also be reduced by drought (McDowell et al. 2009). However, carbohydrate consumption required to maintain cellular metabolism (respiration) will increase due to rising temperatures (Adams et al. 2009; Allen et al. 2009; McDowell et al. 2009), potentially increasing negative effects of drought.

Trees subjected to higher mean temperature showed mean BAI values similar to those of trees growing at milder sites, but long-term BAI declines were stronger in the former. This finding could be interpreted as a sign of temperature-induced drought stress and higher vulnerability to further climate warming. In the 1994 drought event, lower elevation stands showed less drought sensitivity compared with higher elevation trees (Figures 4 and 5). The mean BAI in trees subjected to higher drought stress could reach the minimum survival threshold in the next few years (Bigler and Bugmann 2004). Therefore, the negative BAI trend and lower sensitivity to extreme drought events suggest a higher vulnerability to increasing water deficit (Linares et al. 2009b, 2010). To summarize, the average drought-induced growth limitation remains fairly constant at lower altitude through time (Tiscar 2007), and thus BAI is constrained in the long term (Loustau et al. 2005; Granier et al. 2007). In contrast, in climatically favourable years, trees from moister sites may show higher growth recovery values, as with the detected almost steady or positive BAI trends in the NC, BG, PP, YE and CM stands (see Figures 3 and 5).

In addition to drought, stand age could also play an important role in explaining among-site variance in drought sensitivity and BAI trends (Tiscar 2002, 2007). The BAI trend in old stands seems to be steady (Figure 6), perhaps indicating

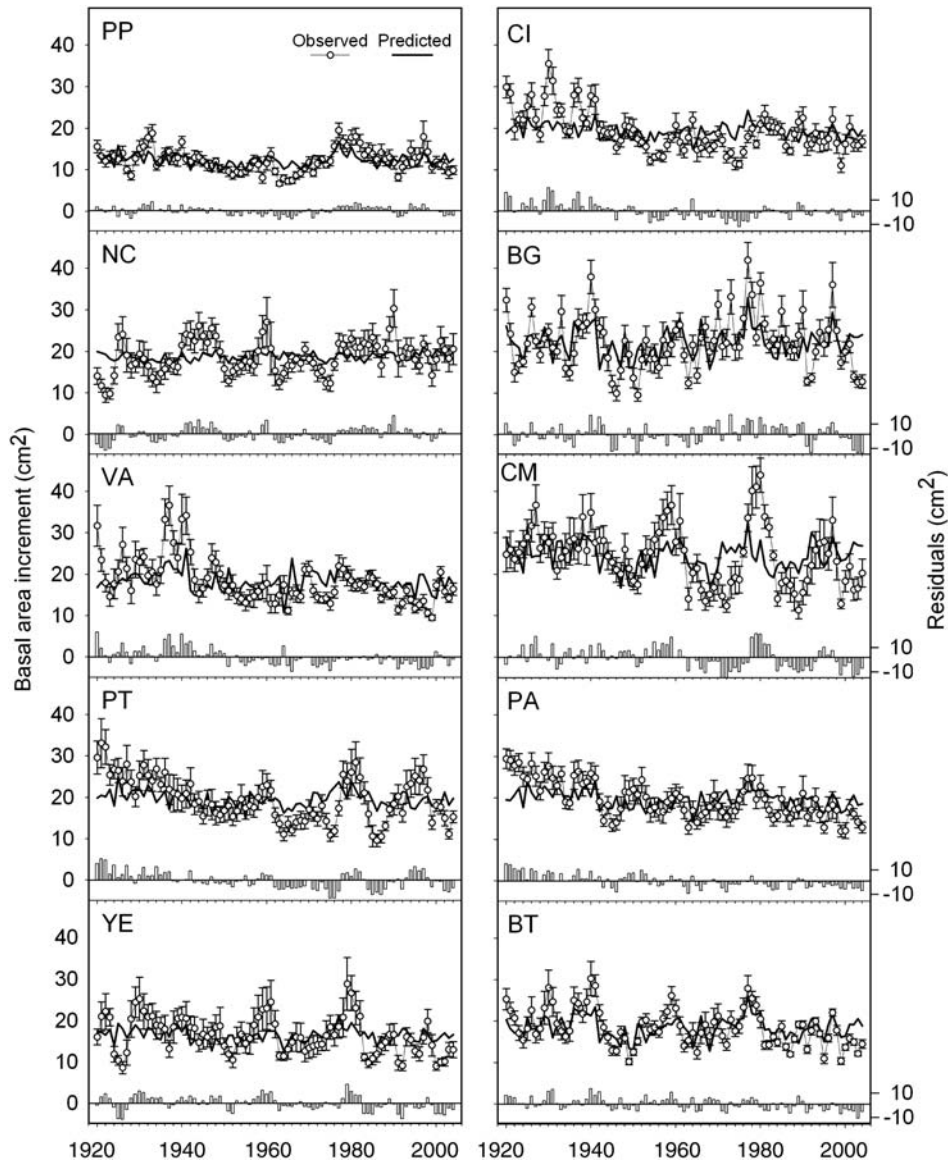


Figure 3. Raw data of BAI (line and scatters) in the 10 studied plots and LMEM (lines) fits based on climatic variables (see Table 4). Bar plots (right axis) indicate the residuals of the LMEM. Error bar represent the standard error from 10 trees per location; one core per tree was studied.

an adaptive capacity that permits old trees to adjust better to new environmental conditions. Older trees have been exposed to long- and short-term environmental changes during their life history and have shown a capability to respond and adapt to (or at least to survive) these changes. In our case, long-term temperature increase represents a gradual directional environmental shift that is interacting with short-term extreme drought events. Both stressors could evolve different adaptation mechanisms, such as acclimation and epigenetic responses (Tognetti et al. 2000, Parmesan 2006). However, the mechanisms underlying these adaptive processes are not yet well understood. The acclimation response over the lifetime of a tree has been observed, for instance, for the gradual

decrease in leaf stomatal density (Wagner et al. 1996). Rapid climate change challenges this process by imposing stronger selection and by distancing populations from environments to which they are adapted. In contrast, local adaptation underlies natural selection, which drives populations towards higher fitness to meet environmental change. In this respect, it is likely that low-altitude populations of *P. nigra* constitute a valuable genetic resource in an environment that is changing towards warmer conditions (Hampe and Petit 2005).

Acknowledgments

The authors are grateful to Dr J. J. Camarero for dendroecological advice. Consejería de Medio Ambiente (Junta de Andalucía) pro-

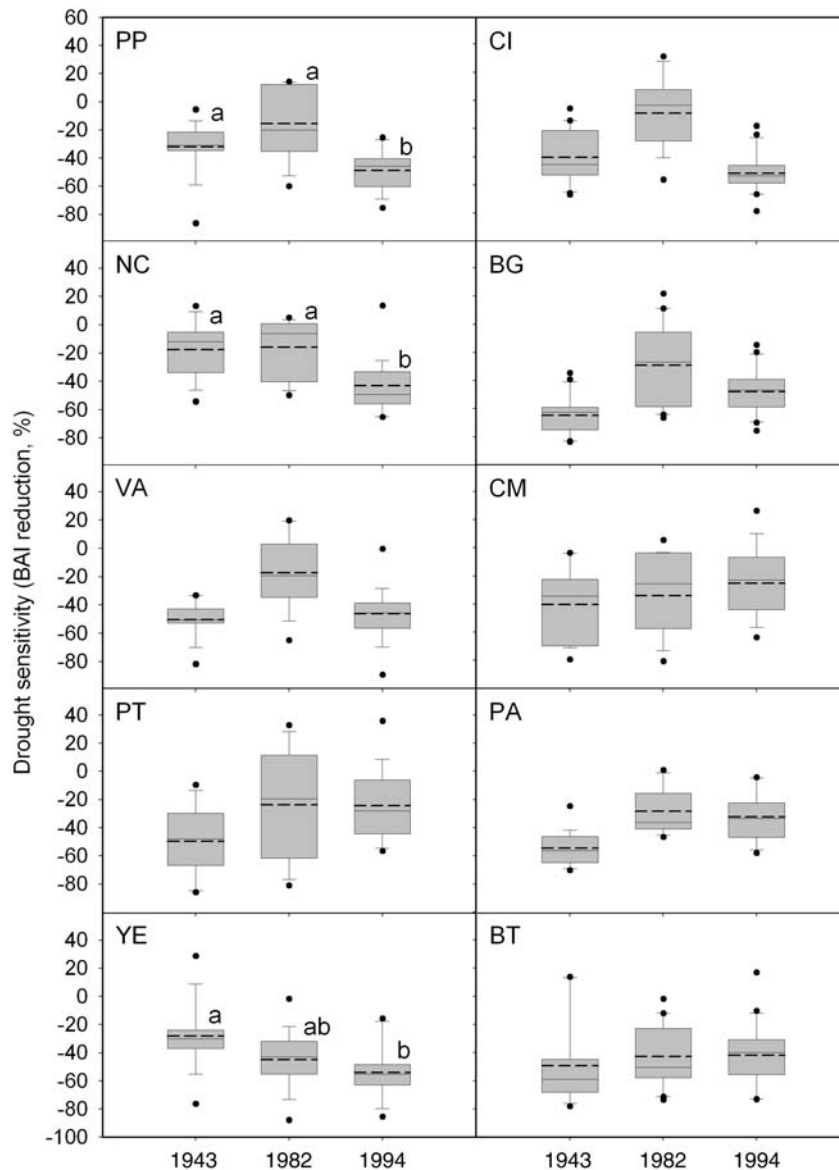


Figure 4. Drought sensitivity estimated as BAI reduction percentage, related to the mean BAI of the decade prior to the droughts registered in 1943, 1982 and 1994. In the box-plot figure, error bars represent the 5th/95th percentiles; boxes represent the standard errors ($n = 10$ trees per plot; one core per tree was studied); solid lines represent the median; dashed lines are the mean values; and points are outliers. Different letters represent significant differences for repeated-measures MANOVA, $P < 0.05$.

vided the means to carry out the field work. We want to thank the comment and suggestions of Sean Thomas and three anonymous reviewers improving a previous version of the manuscript.

Supplementary Data

Supplementary data for this article are available at *Tree Physiology* Online.

References

- Adams, H.D., M. Guardiola-Claramonte, G.A. Barron-Gafford, J.C. Villegas, D.D. Breshears, C.B. Zou, P.A. Troch and T.E. Huxman. 2009. Temperature sensitivity of drought-induced tree mortality: implications for regional die-off under global-change-type drought. *Proc. Natl Acad. Sci. USA* 106:7063–7066.
- Alejano, R. and E. Martínez. 1996. Distribución de *Pinus nigra* Arn. subsp. *salzmannii* en las sierras Béticas. *Ecología* 10:231–241.
- Allen, C.D., A.K. Macalady, H. Chenchouni et al. 2009. A global overview of drought and heat-induced tree mortality reveals emerging climate change risks for forests. *For. Ecol. Manage.* doi: 10.1016/j.foreco.2009.09.001.
- Andreu, L., E. Gutiérrez, M. Macías, M. Ribas, O. Bosch and J.J. Camarero. 2007. Climate increases regional tree-growth variability in Iberian pine forests. *Glob. Change Biol.* 13:1–12.
- Antonova, G.F., V.P. Cherkashin, V.V. Stasova and T.N. Varaksina. 1995. Daily dynamics in xylem cell radial growth of Scots pine (*Pinus sylvestris* L.). *Trees-Struct. Funct.* 10:24–30.

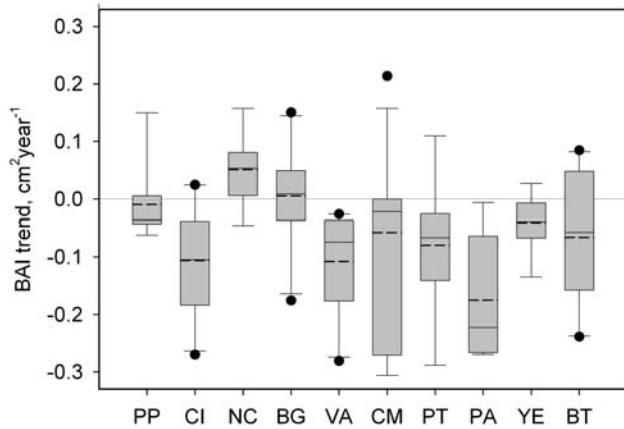


Figure 5. BAI trend estimated for the period 1900–2004. In the boxplot figure, error bars represent the 5th/95th percentiles; boxes represent the standard errors ($n = 10$ trees per plot; one core per tree was studied); solid lines represent the median; dashed lines are the mean values; and points are outliers. Different letters represent significant differences for repeated-measures MANOVA, $P < 0.05$.

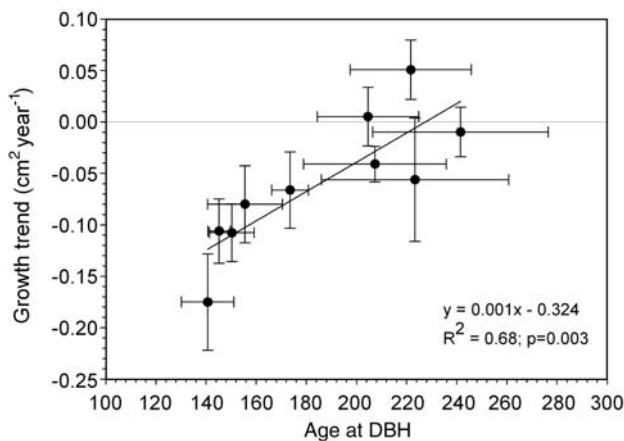


Figure 6. Mean stand age and BAI trends relationship. Error bars represent the standard error from 10 trees per location; one core per tree was studied.

Bigler, C.J. and H. Bugmann. 2004. Predicting the time of tree death using dendrochronological data. *Ecol. Appl.* 14:902–914.

Boisvenue, C. and S.W. Running. 2006. Impacts of climate change on natural forest productivity—evidence since the middle of the 20th century. *Glob. Change Biol.* 12:1–12.

Büntgen, U., D.C. Frank, R.J. Kaczka, A. Verstege, T. Zwijackz-Kozica and J. Esper. 2007. Growth responses to climate in a multi-species tree-ring network in the Western Carpathian Tatra Mountains, Poland and Slovakia. *Tree Physiol.* 27:689–702.

Camarero, J.J., J. Guerrero-Campo and E. Gutiérrez. 1998. Tree-ring growth and structure of *Pinus uncinata* and *Pinus sylvestris* in the Central Spanish Pyrenees. *Arct. Antarct. Alp. Res.* 30:1–10.

De Luis, M., J. Gričar, K. Čufar and J. Raventós. 2007. Seasonal dynamics of wood formation in *Pinus halepensis* from dry and semi-arid ecosystems in Spain. *IAWA J.* 28:389–404.

Deslauriers, A. and H. Morin. 2005. Intra-annual tracheid production in balsam fir stems and the effect of meteorological variables. *Trees-Struct. Funct.* 19:402–408.

Deslauriers, A., H. Morin and Y. Bégin. 2003. Cellular phenology of annual ring formation of *Abies balsamea* (L.) Mill. in the Québec boreal forest (Canada). *Can. J. For. Res.* 33:190–200.

Eilmann, B., P. Weber, D. Rigling and D. Eckstein. 2006. Growth reactions of *Pinus sylvestris* L. and *Quercus pubescens* Willd. to drought years at a xeric site in Valais, Switzerland. *Dendrochronologia* 23:121–132.

Fernández, A., M. Génova, J. Creus and E. Gutiérrez. 1996. Dendroclimatological investigation covering the last 300 years in central Spain. In *Tree Rings, Environment and Humanity*. Eds. J.S. Dean, D.M. Meko and T.W. Swetman. Radiocarbon. U. of Arizona, Tucson, pp 181–190.

Franklin, J.F., H.H. Shugart and M.E. Harmon. 1987. Tree death as an ecological process. *Bioscience* 37:550–556.

Fritts, H.C., E.A. Vaganov, I.V. Sviderskaya and A.V. Shashkin. 1991. Climatic variation and tree-ring structure in conifers: empirical and mechanistic models of tree-ring width, number of cells, cell-size, cell-wall thickness and wood density. *Climate Res.* 1:97–116.

Granier, A., M. Reichstein, N. Bréda et al. 2007. Evidence for soil water control on carbon and water dynamics in European forests during the extremely dry year: 2003. *Agric. For. Meteorol.* 143: 123–145.

Hampe, A. and R.J. Petit. 2005. Conserving biodiversity under climate change: the rear edge matters. *Ecol. Lett.* 8:461–467.

He, J.-S., Q.-B. Zhang and F.A. Bazzaz. 2005. Differential drought responses between saplings and adult trees in four co-occurring species of New England. *Trees-Struct. Funct.* 19:442–450.

Holmes, R.L. 1983. Computer-assisted quality control in tree-ring dating and measurement. *Tree-Ring Bulletin* 43:68–78.

Holmes, R.L. 1992. *Dendrochronology Program Library*. Laboratory of Tree-Ring Research, University of Arizona, Tucson.

IPCC Climate change, fourth assessment report. Cambridge University Press, London, UK.

Keeling, C.D., J.F.S. Chin and T.P. Whorf. 1996. Increased activity of northern vegetation inferred from atmospheric CO₂ measurements. *Nature* 382:146–149.

Kendall, M.G. 1975. *Rank correlation methods*. Charles Griffin, London.

Ko Heinrichs, D., J.C. Tardif and Y. Bergeron. 2007. Xylem production in six tree species growing on an island in the boreal forest region of western Quebec. Canada. *Can. J. Bot.* 85: 518–525.

Laureano, R.G., Y.O. Lazo, J.C. Linares, A. Luque, F. Martínez, J.I. Seco and J. Merino. 2008. The cost of stress resistance: construction and maintenance costs of leaves and roots in two populations of *Quercus ilex*. *Tree Physiol.* 28:1721–1728.

Lebourgeois, F. 2000. Climatic signals in earlywood, latewood and total ring width of Corsican pine from western France. *Ann. For. Sci.* 57:155–164.

Libiseller, C. and A. Grimvall. 2002. Performance of partial Mann Kendall tests for trend detection in the presence of covariates. *Environmetrics* 13:71–84.

Linares, J.C., J.J. Camarero and J.A. Carreira. 2009a. Plastic responses of *Abies pinsapo* xylogenesis to drought and competition. *Tree Physiol.* 29:1525–1536.

Linares, J.C., J.J. Camarero and J.A. Carreira. 2009b. Interacting effects of climate and forest-cover changes on mortality and growth of the southernmost European fir forests. *Global Ecol. Biogeogr.* 18:485–497.

- Linares, J.C., J.J. Camarero and J.A. Carreira. 2010. Competition modulates the adaptation capacity of forests to climatic stress: insights from recent growth decline and death in relict stands of the Mediterranean fir *Abies pinsapo*. *J. Ecol.* 98:592–603.
- Lindner, M., M. Maroschek, S. Netherer et al. 2009. Climate change impacts, adaptive capacity, and vulnerability of European forest ecosystems. *For. Ecol. Manage.* 162:73–86.
- Loustau, D., A. Bosc, A. Colin et al. 2005. Modeling climate change effects on the potential production of French plains forests at the sub-regional level. *Tree Physiol.* 25:813–823.
- Macias, M., L. Andreu, O. Bosch, J.J. Camarero and E. Gutiérrez. 2006. Increasing aridity is enhancing silver fir *Abies alba* (Mill.) water stress in its south-western distribution limit. *Clim. Change* 79:289–313.
- Mann, H.B. 1945. Nonparametric tests against trend. *Econometrica* 13:245–259.
- Martín-Benito, D., P. Cherubini, M. del Río and I. Cañellas. 2007. Growth response to climate and drought in *Pinus nigra* Arn. trees of different crown classes. *Trees* 22:363–373.
- Martínez-Vilalta, J., B.C. López, N. Adell, L. Badiella and M. Ninyerola. 2008. Twentieth century increase of Scots pine radial growth in NE Spain shows strong climate interactions. *Glob. Change Biol.* 14:2868–2881.
- McDowell, N., C.D. Allen and L. Marshall. 2009. Growth, carbon isotope discrimination, and climate-induced mortality across a *Pinus ponderosa* elevation transect. *Glob. Change Biol.* doi:10.1111/j.1365-2486.2009.01994.x.
- Orwig, D.A. and M.D. Abrams. 1997. Variation in radial growth responses to drought among species, site, and canopy strata. *Trees-Struct. Funct.* 11:474–484.
- Parnesan, C. 2006. Ecological and evolutionary responses to recent climate change. *Annu. Rev. Ecol. Evol. Syst.* 37:637–669.
- Peñuelas, J. and I. Filella. 2001. Phenology: responses to a warming world. *Science* 294:793–795.
- Pereira, J.S. and M.M. Chaves. 2001. Plant responses to drought under climate change in Mediterranean-type ecosystems. *Global Change and Mediterranean-Type Ecosystems*. Springer, New York, 140–161.
- Pichler, P. and W. Oberhuber. 2007. Radial growth response of coniferous forest trees in an inner Alpine environment to heat-wave in 2003. *Forest Ecol. Manage.* 242:688–699.
- R Development Core Team 2010. R: a language and environment for statistical computing. R Foundation for Statistical Computing, Vienna, Austria, ISBN 3-900051-07-0, URL <http://www.R-project.org>.
- Richter, K., D. Eckstein and R.L. Holmes. 1991. The dendrochronological signal of pine trees (*Pinus* spp.) in Spain. *Tree Ring Bull.* 51:1–13.
- Rossi, S., A. Deslauriers, T. Anfodillo, H. Morin, A. Saracino, R. Motta and M. Borghetti. 2006b. Conifers in cold environments synchronize maximum growth rate of tree-ring formation with day length. *New Phytol.* 170:301–310.
- Sabaté, S., C. Gracia and A. Sánchez. 2002. Likely effects of climate change on growth of *Quercus ilex*, *Pinus halepensis*, *Pinus pinaster*, *Pinus sylvestris* and *Fagus sylvatica* forests in the Mediterranean Region. *For. Ecol. Manage.* 162:23–37.
- Schröter, D., W. Cramer, R. Leemans et al. 2005. Ecosystem service supply and vulnerability to global change in Europe. *Science* 310:1333–1337.
- Sumner, G., R. Romero, V. Homar, C. Ramis, S. Alonso and E. Zorita. 2003. An estimate of the effects of climate change on the rainfall of Mediterranean Spain by the late twenty first century. *Clim. Dyn.* 20:789–805.
- Tardif, J., J.J. Camarero, M. Ribas and E. Gutiérrez. 2003. Spatiotemporal variability in tree growth in the Central Pyrenees: climatic and site influences. *Ecol. Monogr.* 73:241–257.
- Tíscar, P.A. 2002. Capacidad reproductiva de *Pinus nigra* subsp. *salzmannii* en relación con la edad de la planta madre. *Invest. Agr.: Sist. Recur. For.* 11:357–371.
- Tíscar, P.A. 2007. Dinámica de regeneración de *Pinus nigra* subsp. *salzmannii* al sur de su área de distribución: etapas, procesos y factores implicados. *Inv. Agr.: Sis. Recur. For.* 16:124–135.
- Tognetti, R., P. Cherubini and J.L. Innes. 2000. Comparative stem-growth rates of Mediterranean trees under background and naturally enhanced ambient CO₂ concentrations. *New Phytol.* 146:59–74.
- Vaganov, E.A., M.K. Hughes and A.V. Shashkin. 2006. Growth dynamics of conifer tree rings: images of past and future environments. Springer, Berlin-Heidelberg.
- von Ende, C.N. 2001. Repeated-measures analysis: growth and other time-dependent measures. *In* Design and Analysis of Ecological Experiments. Eds. S.M. Scheiner and J. Gurevitch. Oxford University Press, Oxford, UK, pp 134–157.
- Wagner, F., R. Below, P.D. Klerk, D.L. Dilcher, H. Joosten, W.M. Kürschner and H. Visscher. 1996. A natural experiment on plant acclimation: lifetime stomatal frequency response of an individual tree to annual atmospheric CO₂ increase. *Proc. Natl Acad. Sci. USA* 21:11705–11708.
- Willmott, C.J., C.M. Rowe and Y. Mintz. 1985. Climatology of the terrestrial seasonal water cycle. *Int. J. Climatol.* 5:589–606.
- Wullschleger, S.D., T.J. Tschaplinski and R.J. Norby. 2002. Plant water relations at elevated CO₂—implications for water-limited environments. *Plant Cell Environ.* 25:319–331.
- Zuur, A.F., E.N. Ieno, N. Walker, A.A. Saveliev and G.M. Smith. 2009. Mixed effects models and extensions in ecology with R. Springer, New York.